On the gas-sensing mechanism of resistive based SnO_2 QD gas Sensor

Shambhu Sharan Kumar Sinha
University of Engineering and Management, Kolkata,India
ShambhuSharanKumar.Sinha@uem.edu.in

Sunita Sinha
Government Engineering College, Sheikhpura, India

Sohom Chakraborty
University of Engineering and Management, Kolkata, India

Nivedita Saha
University of Engineering and Management, Kolkata,India

Suparna Mitra
University of Engineering and Management, Kolkata,India

Ankita Deogharia
University of Engineering and Management, Kolkata,India

Soumi Chattopadhyay
University of Engineering and Management, Kolkata,India

Dhiraj Mahato
University of Engineering and Management, Kolkata,India

Utsha Saha
University of Engineering and Management, Kolkata,India

***Abstract*—Tin oxide (SnO2) finds extensive application in metal-oxide-semiconductor systems as a gas-sensing material, owing to its distinct physical and chemical attributes. Among these attributes, grain size stands out as a pivotal factor that significantly shapes the gas- sensing properties. An all-encompassing model is introduced, encompassing the complete spectrum of gas-sensing processes involving receptor function, transducer function, and utility factor. The characteristics of the sensor are defined as dependent on factors such as grain size, width of the depletion layer, thickness of the film, density of oxygen vacancies, concentration of gas, pore dimensions, and operational temperature. This model offers a thorough mathematical elucidation of the impact of SnO2's size variations, spanning from partial depletion to volume depletion.**

Keywords*— Gas Sensor, Tin oxide, Quantum Dot, Sensing Response

I. INTRODUCTION

In the past ten years, there has been a notable rise in the emphasis placed on air quality. The need for technologically advanced sensors is experiencing substantial growth, resulting in a rapid expansion of the gas sensor market. Gas sensors play a critical role in detecting gas leaks [1], ensuring public safety [2], and aiding in medical diagnoses [3]. Among the diverse array of gas sensors available, significant attention has been directed toward tin oxide (SnO2) gas sensors due to their uncomplicated design [4], straightforward manufacturing process, cost-effectiveness, and consistent chemical properties [5]. Presently, room temperature gas sensors hold significant appeal due to their lack of heating elements, contributing to energy efficiency and mitigating explosive risks. SnO2 possesses a wide bandgap and exhibits n-type semiconductor behaviour, adopting the rutile structure with octahedral coordination. As an innovative functional semiconductor, quantum dots (QDs) of SnO2 exhibit unique traits such as small grain size (< 10 nm) and an expanded specific surface area. This results in a substantial exchange of electrons between a considerable number of atoms and gas molecules ad- sorbed on the surface. The gas-sensing characteristics of these QDs hinge on their grain size, showcasing a notable influence stemming from their size [6]. The influence of grain size on the gas-sensing attributes of semiconductor sensors has captivated significant attention from the scientific community. Researchers have effectively elucidated the underlying sensing mechanism from a theoretical perspective. C. Xu introduced a neck-controlled model, dis- closing that the sensor's response peaked when the grain radius (r) closely aligned with the width of the depletion layer (w) [7]. Conversely, the response displayed an inverse relation- ship with grain size when r exceeded w by a substantial margin. However, the aspect of the entire grain achieving volume depletion status wasn't addressed for cases where the grain radius was smaller than the depletion layer width ($r < w$).

Moreover, Yamazoe introduced an all-encompassing framework for semiconductor gas sensors, encompassing the receptor function, the transducer function, and the utility factor[8]. The receptor function addressed the individual crystal's reaction to the target gas under investigation, while the transducer function cantered on the conversion of each crystal's response into device resistance. The utility factor elucidated the dampening of device response (alteration in resistance) within a real porous sensing structure due to the consumption of stimulant gas during its internal diffusion. Hence, as a crucial facet of the receptor function, the impact of grain size became notably significant over the past decade, particularly during the rise of nanomaterials in advanced electronic devices.

This work integrates the receptor function, transducer function, and utility factor to develop an all-encompassing mathematical model. This model is utilized to examine the influence of size on the gas-sensing characteristics of semiconductor grains, spanning from partial depletion to volume depletion. The validity of this proposed model is additionally confirmed through experimental findings.

II. COMPREHENSIVE MATHEMATICAL MODEL FOR THIN FILM GAS SENSORS

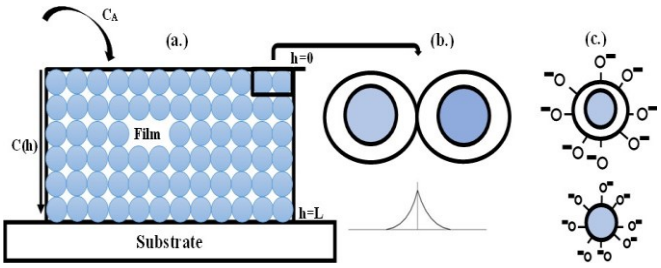

Fig. 1. Gas-sensing mechanism of SnO2 QD resistive based gas sensor: (a) the utility fac- tor, (b) the transducer function and (c) the receptor function of partial depleted and volume depleted grains.

The gas-sensing process within a semiconductor gas sensor comprises three key com- ponents: the receptor

function, transducer function, and utility factor [9]. The utility factor characterizes the diminished response within the sensing body due to the consumption of stimulant gas during its progression through the film's interior [10]. As depicted in Figure 1(a), the thin film consists of an aggregation of SnO2 quantum dots (QDs). Upon exposure to a reducing environment with a concentration denoted as CA, the reducing gas permeates the film by infiltrating the gaps between the grains, adhering to Knudsen diffusion principles. The diffusion equation can be formulated as follows [11].

$$C(h)=\frac{\cosh\left[(L-h)\sqrt{K_c/D_k}\right]}{\cosh\left(L\sqrt{K_c/D_k}\right)} \tag{1}$$

$$D_k=\frac{4r_p}{3}\sqrt{\frac{2G_cT}{\pi M}} \tag{2}$$

The Knudsen diffusion constant (DK) is determined by factors such as temperature (T), the radius of the pores (rp), and the molecular weight (M) of the gas that is diffusing. The gas constant is denoted as Gc [12]. The distribution of gas concentration within a thin film is influenced by parameters like the thickness of the film (L), the distance from the film's surface (h), and a reaction constant (Kc). The transducer function is focused on establishing a connection between two individual grains, converting the response of each grain into measurable electrical properties. This conversion is typically described using the concept of a Schottky barrier, as depicted in Figure 1(b). On the other hand, the receptor function explains how a single grain responds when it is stimulated by an external source, as shown in Figure 1(c). The grains possess inherent oxygen vacancies, which result in quasi-free electrons after ionization. These electrons are then captured by the oxygen adsorbed on the surface, leading to the creation of a depletion layer [13].

The presence of ionized oxygen vacancies creates a Schottky barrier within the region that has experienced depletion. Previous experimental assessments have determined that the width of this depletion layer is approximately 4.2 nm [14, 15]. Consequently, when the grain radius surpasses this width (r > w), the grain becomes partially depleted. Conversely, when the grain's radius is smaller than the depletion layer width (r < w), the entire grain undergoes volume depletion. The total resistance of a grain (Ra) consists of the combined resistances of both the bulk of the grain (Rb) and the depletion layer (Rgb). If we represent Ra(h) as the resistance of a SnO2 grain positioned at a depth h within the thin film, it can be expressed as follows:

$$R_a(h)=R_b+R_{gb}=\rho_0\frac{2(r-w)}{A}+\rho_{gb}\frac{2w}{A} \tag{3}$$

ρ0 and ρgb represent the resistivities of the grain's bulk and the depletion layer, respectively. The term r refers to the grain radius, and w represents the width of the depletion layer. Additionally, A signifies the effective area for electron tunneling at the boundaries between grains. The resistivity of the grain bulk (ρ0) is alternatively known as the flat-band resistivity and can be computed using Equation (4).

$$\rho_0=\frac{1}{nqu} \tag{4}$$

Here, n represents the electron density, q stands for the elemental charge, and μ signifies the electron mobility. The resistivity ρgb exhibits an exponential relationship with ρ0 and both contribute to the overall resistivity of a grain. While in partially depleted grains, ρgb takes precedence, the influence of ρ0 cannot be dismissed in grains exhibiting volume depletion [16, 17]. The connection between the barrier height of the depletion layer, denoted as V(x) and the space charge density, represented as σa(x) is described by the Poisson equation, as shown in Equation (5) [18].

$$\frac{\partial^2V(x)}{\partial x^2}=\frac{-\sigma_a(x)}{\varepsilon} \tag{5}$$

The symbol ε denotes the dielectric constant. The presence of space charge within the depletion layer is influenced by the oxygen vacancies. These innate imperfections have been demonstrated to exhibit a gradient distribution within a semiconductor grain, as evidenced by previous studies [19-21]. However, in minuscule crystalline structures like quantum dots (QDs), the gradient is sufficiently minimal that it is reasonable to assume the distribution of oxygen vacancies is uniform [8]. Consequently, the charge density within the depletion layer can be formulated using Equation (6).

$$\sigma_a(x)=qN_d \tag{6}$$

Here, Nd represents the concentration of oxygen vacancies, which is presumed to be ionized in a first-order manner. The Schottky barrier height described in Equation (8) can be de- rived by applying the boundary conditions outlined in Equation (7).

$$\begin{cases}V(w)=0\\V'(w)=0\end{cases} \tag{7}$$

$$qV_a(x)=\frac{q^2N_d}{2\varepsilon}(x-w)^2 \quad 0<x<w \tag{8}$$

The calculations for the barrier height at the grain boundary and the resistivity of the depletion layer (ρgb) are performed using Equations (9) and (10), respectively.

$$qV_{sa}=qV_a(0)=\frac{q^2w^2N_d}{2\xi} \tag{9}$$

$$\rho_{gb}=\rho_0\exp\left(\frac{qV_{sa}}{KT}\right)=\rho_0\exp\left(\frac{W^2}{2L_D^2}\right) \tag{10}$$

$$L_D=\sqrt{\xi KT/q^2N_d} \tag{11}$$

Here, K signifies the Boltzmann constant, while T denotes the temperature. The concept of the Debye length (L_D) is introduced in Equation (11) [22]. Consequently, the formulation for the total resistance R_a can be represented as given in Equation (12).

$$R_a = \int_0^L R_a(h)\partial h = \frac{2\rho_0 L}{A}\left[r - w + w\exp\left(\frac{w^2}{2L_D^2}\right)\right] \quad (12)$$

In an environment with a reducing atmosphere, the resistance of an individual SnO2 quantum dot (QD) grain (Rg) is comprised of the combined resistances from the grain's bulk (Rb) and the depletion layer (Rgb'). Correspondingly, Rg(h) represents the resistance of a SnO2 grain situated at a depth h within the thin film. This resistance can be expressed using Equation (13).

$$R_g(h) + R_b + R_{gb'} \quad (13)$$

The dispersion of electrons (nR) released back into the depletion layer following gas expo- sure exhibits an essentially uniform distribution. It is posited that this distribution is directly proportional to the concentration of oxygen vacancies (Nd), as outlined in Equation (14).

$$n_R = \alpha N_d \quad (14)$$

The parameter α indicates the percentage of captured electrons that are returned to the depletion layer. Its value ranges from 0 (in the presence of air) to 1 (in a vacuum or an atmosphere devoid of oxygen), and it is correlated with the partial pressure of oxygen or the presence of reducing gas [23]. Consequently, when the thin film is exposed to a reducing gas, a connection can be established between the space charge density σg(x) and the concentration of oxygen vacancies Nd. This relationship is illustrated by Equation (15).

$$\sigma_g(x) = q(N_d - n_R) = (1-\alpha)qN_d \quad (15)$$

In a similar manner, the calculation of the barrier height at the grain boundary and the resistivity of the depletion layer (ρgb) is achieved using the Poisson equation, as expressed in Equations (16) and (17).

$$qV_{sg} = qV_g(0) = \frac{(1-\alpha)q^2w^2N_d}{2\xi} \quad (16)$$

$$\rho_{gb'} = \rho_0 \exp\left(\frac{qV_{sg}}{KT}\right) = \rho_0 \exp\left[(1-\alpha)\frac{w^2}{2L_D^2}\right] \quad (17)$$

For the sake of analysis, let's assume that the adsorbed oxygen exists in the form of [O-] [9], which is capable of capturing electrons on the surface of the grain. Additionally, considering that the oxygen vacancies act as donors and are uniformly distributed, we arrive at the following equations as presented in Equation (18).

$$[O^-] = N_d w \quad (18)$$

The concentration of liberated electrons within the depletion layer, denoted as [e-], can be formulated according to Equation (19)

$$[e^-] = \alpha N_d \quad (19)$$

Upon exposure of the sensor to C_4H_{10}, the gas molecules undergo reactions with the oxygen that is adsorbed on the surface. These reactions are commonly represented by Equations (20) and (21).

$$O_2 + 2e^- \underset{k_{-1}}{\overset{k_1}{\rightleftharpoons}} 2O^- \quad (20)$$

$$C_4H_{10} + 13O^- \xrightarrow{K_2} 4CO_2 + 5H_2O + 13e^- \quad (21)$$

In this context, k1, k-1, and k2 represent the rate constants of the reactions. The reverse process of Equation (20) occurs at a comparatively slower rate and can therefore be disregarded. As a result, the rate at which [O-] accumulates is expressed using Equation (22)

$$\frac{\partial[O^-]}{\partial t} = K_1P_{O_2}[e^-]^2 - K_{-1}[O^-]^2 - K_2P_{C_4H_{10}}[O^-]^{13} \quad (22)$$

In this scenario, Po2, signifies the concentration of O2, while PC4H10, represents the concentration of C4H10. When the system reaches a steady state, Equations (20) and (21) attain equilibrium in accordance with the derived Equations (23) and (24).

$$K_1P_{O_2}[e^-]^2 - K_2P_{C_4H_{10}}[O^-]^{13} = 0 \quad (23)$$

$$\alpha = \left(\frac{K_2N_d^{11}w^{13}}{K_1P_{O_2}}\right)^{0.5}\left(P_{C_4H_{10}}\right)^{0.5} = \beta[C(h)]^{0.5} \quad (24)$$

The symbol β denotes the coefficient of proportionality. As a result, the expression for the resistance of a SnO_2 grain at a depth h denoted as Rg(h), can be formulated according to Equation (25).

$$R_g(h) = \frac{2\rho_0}{A}\left\{r - w + w\exp\left[\left(1-\beta[C(h)]^{0.5}\right)\frac{w^2}{2L_D^2}\right]\right\} \quad (25)$$

Therefore, the expression for R_g can be found as Equation (26).

$$R_g = \frac{2\rho_0 L}{A}\left\{r - w + \frac{4L_D^2}{wm}\exp\left(\frac{w^2}{2L_D^2}\left(1-\beta C_A^{0.5}\right)\left[\exp\left(\frac{mw^2}{4L_D^2}\right)-1\right]\right)\right\} \quad (26)$$

$$m = \beta C_A^{0.5} L\sqrt{\frac{K_c}{D_k}}\tanh\left(L\sqrt{K_c/D_k}\right) \quad (27)$$

Here, the parameter m is introduced straightforwardly in the equation. When the grain's radius exceeds the depletion layer width (r > w), the grain experiences partial depletion. As a result, the sensor's response is derived as described in Equation (28).

$$S = \frac{r - w + w\exp\left(w^2/2L_D^2\right)}{r - w + \frac{4L_D^2}{wm}\exp\left(\frac{w^2}{2L_D^2}\left(1-\beta C_A^{0.5}\right)\left[\exp\left(mw^2/4L_D^2\right)-1\right]\right)} \quad (28)$$

The response of volume-depleted grain is formulated as Equation (29).

$$S = \frac{r^2 m\exp\left(\frac{r^2}{2L_D^2}\beta C_A^{0.5}\right)}{4L_D^2\left[\exp\left(mr^2/4L_D^2\right)-1\right]} \quad (29)$$

III. RESULTS AND DISCUSSIONS

Consequently, based on the comprehensive mathematical model for gas sensing in semi- conductors, a series of mathematical simulations were conducted utilizing the following parameters: dielectric constant (ε) set at 8.85×10^{-10} F/m, proportional coefficient (β) at 0.005 $ppm^{-0.5}$, reaction constant (k_c) at 10,000 mol/(L s), depletion layer width (w) fixed at 4 nm [24, 25], elemental charge (q) at 1.6×10^{-19} C, concentration of oxygen vacancies (N_d) set to.

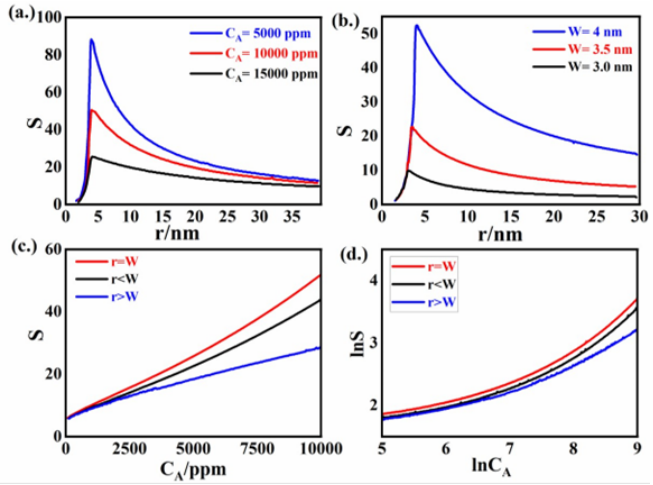

Fig. 2. Simulation results of theoretical model: the relationship between sensor response and (a) grain size at various concentrations, (b) grain size at various depletion layer widths, (c) gas concentration in linear coordinates, (d) gas concentration in logarithmic coordinates.

8.5×10^{25} m^{-3} [22], Boltzmann constant (k) at 1.38×10^{-23} J/K [26], and gas constant (Gc) at 8.314 J/(mol K) [27]. The remaining parameters are configured to align with experimental conditions: temperature (T) is 298 K, gas concentration (CA) is 10,000 ppm, and the film thickness (L) is 381 nm. Volume-depletion and partial-depletion grain sizes are defined as 3.9 nm and 10 nm, respectively. The resulting trends are depicted in Figure 2(a), illustrating the sensor response's negative correlation with grain size when r > w. The response reaches its maximum at r = w and subsequently diminishes with further reduction in grain size. This finding corroborates the anticipated size effect from the gradient-distributed oxygen vacancies model [19]. Consequently, the value of the depletion layer width (w) proves to be pivotal in determining semiconductor sensor performance. Previous studies have approximated the value of w to range between 3 and 4.2 nm [15, 28]. The impact of w on the sensor response is graphically presented in Figure 2(b), revealing that the response peak consistently aligns with r = w, with response magnitude increasing alongside the depletion layer. Lastly, Figures 2(c) and 2(d) elucidate the influence of gas concentration on sensor response, depicted in both linear and logarithmic coordinates, respectively.

IV. CONCLUSIONS

A detailed mathematical model has been formulated to describe the behavior of semiconductor gas sensors, considering elements such as the receptor function, transducer function, and utility factors. Through simulations, it has been observed that the sensor response achieves its maximum value when the grain radius matches the depletion layer width. The relationships between sensor response and factors like gas concentration, film thickness, operational temperature, ionized donor density, and pore radius have been quantified. These simulation outcomes have been validated against real-world experimental thin film gas sensors, indicating the strong suitability and effectiveness of the mathematical model for describing the behavior of semiconductor gas sensors.

ACKNOWLEDGMENT

I would like to express my sincere gratitude and appreciation to University of Engineering and Management Kolkata for providing access to their laboratory facilities and resources, which were vital for conducting experiments and data collection.

REFERENCES

[1] X.F. Liu, H.P. Dong, S.H. Xia, Micromachined catalytic combustible hydrogen gas sensor based on nano-structured SnO2, Acta Chim. Sin. 71 (2013) 657–662.

[2] V. Krivetskiy, K. Zamanskiy, A. Beltyukov, A. Asachenko, M. Topchiy, M. Nechaev,A. Garshev, A. Krotova, D. Filatova, K. Maslakov, M. Rumyantseva, A. Gaskov, Effect of AuPd bimetal sensitization on gas sensing performance of nanocrystalline sno2 obtained by single step flame spray pyrolysis, Nanomaterials 9 (2019) 728.

[3] A.A. Vasiliev, A.E. Varfolomeev, I.A. Volkov, N.P. Simonenko, P.V. Arsenov,I.S. Vlasov, V.V. Ivanov, A.V. Pislyakov, A.S. Lagutin, I.E. Jahatspanian, T. Maeder, Reducing humidity response of gas sensors for medical applications: use of spark discharge synthesis of metal oxide nanoparticles, Sensors 18 (2018) 2600.

[4] Y. Fu, J. Li, H. Xu, SnO2 recycled from tin slime for enhanced SO2 sensing properties by NiO surface decoration, Mater. Sci. Semicond. Process. 114 (2020) 105073.

[5] O. Kendall, P. Wainer, S. Barrow, J. van Embden, E. Della Gaspera, Fluorine-doped tin oxide colloidal nanocrystals, Nanomaterials 10 (2020) 863.

[6] H. Liu, S. Xu, M. Li, G. Shao, H. Song, W. Zhang, W. Wei, M. He, L. Gao, H. Song,J. Tang, Chemiresistive gas sensors employing solution-processed metal oxide quantum dot films, Appl. Phys. Lett. 105 (2014) 163104.

[7] X. Chaonan, T. Jun, M. Norio, Y. Noboru, Relationship between gas sensitivity and microstructure of porous SnO2, Denki KagaKu 58 (1990) 1143–1148.

[8] N. Yamazoe, K. Shimanoe, New perspectives of gas sensor technology, Sens. Actuators B: Chem. 138 (2009) 100–107.

[9] N. Yamazoe, J. Fuchigami, M. Kishikawa, T. Seiyama, Interactions of tin oxide surface with O2, H2O and H2, Surf. Sci. 86 (1979) 335–344.

[10] G. Sakai, N. Matsunaga, K. Shimanoe, N. Yamazoe, Theory of gas-diffusion controlled sensitivity for thin film semiconductor gas sensor, Sens. Actuators B: Chem. 80 (2001) 125–131.

[11] G. Sakai, N. Matsunaga, K. Shimanoe, N. Yamazoe, Theory of gas-diffusion controlled sensitivity for thin film semiconductor gas sensor, Sens. Actuators B: Chem. 80 (2001) 125–131.

[12] N. Matsunaga, G. Sakai, K. Shimanoe, N. Yamazoe, Diffusion equation-based study of thin film semiconductor gas sensor-response transient, Sens. Actuators B: Chem. 83 (2002) 216–221.

[13] S.R. Morrison, Mechanism of semiconductor gas sensor operation, Sens. Actuators 11 (1987) 283–287.

[14] J. Liu, Z. Zhai, G. Jin, Y. Li, F.F. Monica, X. Liu, Simulation of the grain size effect in gas-sensitive SnO2 thin films using the oxygen vacancy gradient distribution model, Electron. Mater. Lett. 11 (2015) 34–40.

[15] J. Liu, X. Liu, Z. Zhai, G. Jin, Q. Jiang, Y. Zhao, C. Luo, L. Quan, Evaluation of deple- tion layer width and gas-sensing properties of antimony-doped tin oxide thin film sensors, Sens. Actuators B: Chem. 220 (2015) 1354–1360..

[16] J. Liu, J. Lv, J. Shi, L. Wu, N. Su, C. Fu, Q. Zhang, Size effects of tin oxide quantum dot gas sensors: from partial depletion to volume depletion, J. Mater. Res. Technol. 9 (2020) 16399–16409.

[17] C. Xu, J. Tamaki, N. Miura, N. Yamazoe, Grain size effects on gas sensitivity of porous SnO2-based elements, Sens. Actuators B 3 (1991) 147–155.

[18] J. Liu, Y. Gao, X. Wu, G. Jin, Z. Zhai, H. Liu, Inhomogeneous oxygen vacancy distribu- tion in semiconductor gas sensors: formation, migration and determination on gas sensing characteristics, Sensors 17 (2017) 1852.

[19] J. Liu, S. Gong, L. Quan, Z. Deng, H. Liu, D. Zhou, Influences of cooling rate on gas sensitive tin oxide thin films and a model of gradient distributed oxygen vacancies in SnO2 crystallites, Sens. Actuators B: Chem. 145 (2010) 657–666.

[20] J. Liu, Y. Gao, X. Wu, G. Jin, Z. Zhai, H. Liu, Inhomogeneous oxygen vacancy distribu- tion in semiconductor gas sensors: formation, migration and determination on gas sensing characteristics, Sensors 17 (2017) 1852.

[21] J. Liu, S. Gong, Q. Fu, Y. Wang, L. Quan, Z. Deng, B. Chen, D. Zhou, Time-dependent oxygen vacancy distribution and gas sensing characteristics of tin oxide gas sensitive thin films, Sens. Actuators, B 150 (2010) 330–338.

[22] N. Yamazoe, K. Shimanoe, Theory of power laws for semiconductor gas sensors, Sens. Actuators B: Chem. 128 (2008) 566–573.

[23] J. Liu, S. Gong, L. Quan, Z. Deng, H. Liu, D. Zhou, Influences of cooling rate on gas sensitive tin oxide thin films and a model of gradient distributed oxygen vacancies in SnO2 crystallites, Sens. Actuators B: Chem. 145 (2010) 657–666.

[24] J. Liu, S. Gong, L. Quan, Z. Deng, H. Liu, D. Zhou, Influences of cooling rate on gas sensitive tin oxide thin films and a model of gradient distributed oxygen vacancies in SnO2 crystallites, Sens. Actuators B: Chem. 145 (2010) 657–666.

[25] C. Xu, J. Tamaki, N. Miura, Relationship between gas sensitivity and microstructure of porous SnO2, Denki Kagaku oyobi Kogyo Butsuri Kagaku 58 (1990) 1143–1148.

[26] B. Fellmuth, C. Gaiser, J. Fischer, Determination of the Boltzmann constant-status and prospects, Meas. Sci. Technol. 17 (2006) R145–R159.

[27] MichaelJ. Moran, Fundamentals of Engineering Thermodynamics, 4th ed., J. Wiley & Sons, 2000.

[28] J. Liu, X. Liu, Z. Zhai, G. Jin, Q. Jiang, Y. Zhao, C. Luo, L. Quan, Evaluation of deple- tion layer width and gas-sensing properties of antimony-doped tin oxide thin film sensors, Sens. Actuators B: Chem. 220 (2015) 1354–1360.